Large-scale morphology of Arctic continental slopes: the influence of sediment delivery on slope form

DAMIAN B. O'GRADY* & JAMES P. M. SYVITSKI

Institute of Arctic and Alpine Research, University of Colorado, Boulder, Colorado, 80309-0450, USA (e-mail: damian.ogrady@colorado.edu)

**Present address: Exxon Mobil Upstream Research Company, P.O. Box 2189, Houston TX 77252 (e-mail: damian.b.ogrady@exxonmobil.com)*

Abstract: The continental slopes of the pan-Arctic region exhibit a range of morphological expression inherently related to different styles of glaciation and sediment delivery to the slope. This study examines the basic associations between glacial processes and morphology at the regional scale. A Geographical Information System (GIS) is applied to a new bathymetric grid of the Arctic Ocean in order to compare the slope angle and sea-floor roughness of 70% of Arctic continental slopes. We also subdivide the circum-Arctic continental slope with respect to parameters likely to influence sediment delivery to the slope. These include proximity to Late Quaternary glacial advance, convergent versus divergent ice termini, and the presence or absence of glacial shelf troughs. Comparison shows that those continental slopes that experience higher sediment input dip more gently than slopes with less sediment input. On glaciated margins where the expanding ice sheet would have produced convergent (faster) ice flow, continental slopes have mean slopes of 1.3° on average. This is in contrast with margins that have experienced divergent (slower) ice flow which tend to have steeper slopes (mean of 2.2°). There is a direct relationship between morphological variability among trough-mouth fans and the width of the adjacent continental shelf (i.e. size of the trough). Longer troughs give rise to slope fans with a more gentle profile geometry. This finding, though simple, suggests a dependency of slope morphology on sediment input to the slope through basal ice sheet erosion. Published values for sediment discharge to several trough mouth fans support this concept. A model is proposed for fan development that relates a fan's geomorphic state to its stage of stratigraphic development.

Introduction

Recent studies show that the morphology of high-latitude continental slopes can vary considerably between regions of recent glacial advance (Vorren and Laberg 1997; Dowdeswell *et al.* 1998; Taylor *et al.* 2000). Such variations seem to reflect diversity in the mechanisms and rates of sediment delivery to the margin by glacial termini (Fig. 1; Dowdeswell *et al.* 1996). Understanding the link between sedimentary processes and morphology of continental slopes begins with recognizing diversity in sedimentary environments and the resultant morphology. Our current understanding of this link for the Arctic glacial system stems from a small number of well-studied continental margins for which ample data on morphology and sedimentary processes exist. Examples include Arctic trough mouth fans (Laberg & Vorren 1996*a*); the canyon-dissected northern Norway margin (Taylor *et al.* 2000); and the turbidite-dominated southern Greenland margin (Hesse *et al.* 1999). Such examples highlight the associations between glacial process and slope morphology because they represent ends-of-the-spectrum in terms of glacial margin sedimentary systems. For example, high sediment delivery from trough–mouth systems (Elverhøi *et al.* 1998) commonly leads to a low-angle, debris-flow dominated fan. In contrast, sediment starved regions may be more prone to canyon development such as in the Norwegian Andøya margin (Taylor *et al.* 2000). It is unclear whether such associations are relevant only to these end-member systems or whether they may be applied to all high-latitude slopes.

The purpose of this study is to understand whether a systematic relationship exists between glacial processes and continental slope morphology for the entire range of northern high-latitude margins. To address this problem we compare the large-scale continental slope morphology for several regions of the Arctic covering a broad spectrum of glacial to non-glacial sedimentary environments.

From: DOWDESWELL, J. A. & Ó COFAIGH, C. (eds) 2002. *Glacier-Influenced Sedimentation on High-Latitude Continental Margins.* Geological Society, London, Special Publications, **203**, 11–31. 0305-8719/02/$15.00

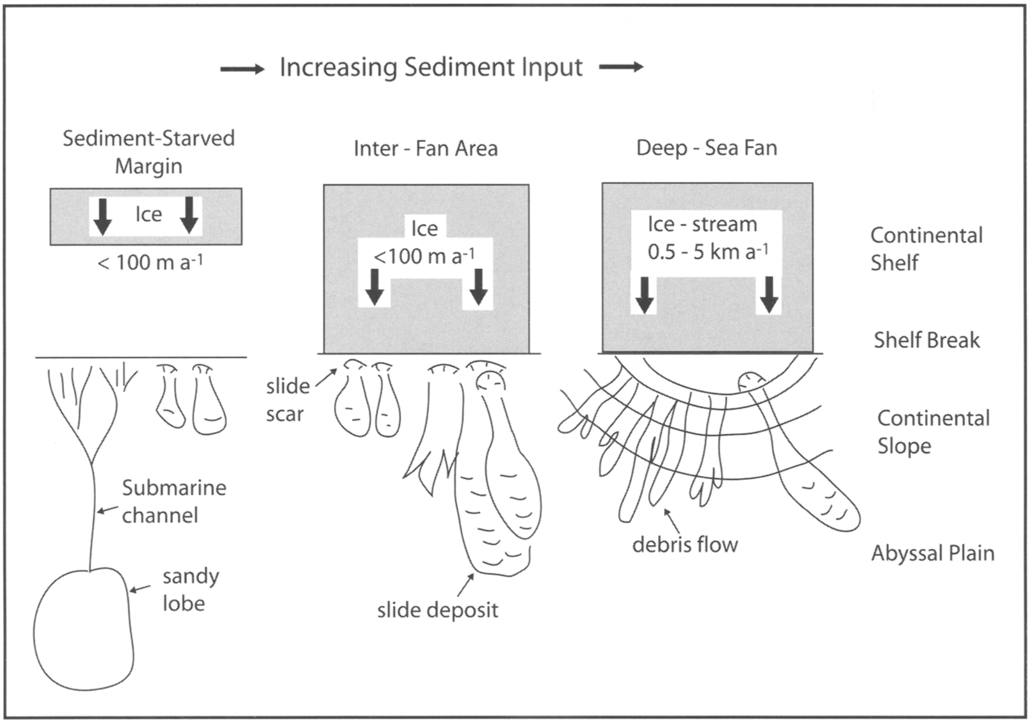

Fig. 1. Conceptual model showing the change in the style of slope deposition in relation to ice proximity and rate of glacial sedimentation (Dowdeswell *et al.* 1996).

Arctic bathymetry

Due to a lack of suitable bathymetric data, regional comparisons of Arctic slope morphology have lagged behind those of more temperate regions (i.e. O'Grady *et al.* 2000; Adams & Schlager 2000). Consequently, most previous comparisons of Arctic slope morphology are limited to only the best studied margins (Laberg & Vorren 1996*a*). In this study we use the recent International Bathymetric Chart of the Arctic Ocean (IBCAO; Jakobsson *et al.* 2000); a compilation and fusion of digitized soundings and contours from a variety of contributing sources. The grid is 6000 × 6000 km with 2.5 km cell spacing in a Cartesian coordinate system and a Polar stereographic projection (true scale at 75°N). The IBCAO covers all of the Arctic Ocean and adjacent shelf seas as well as most of the Labrador, Norwegian, and Greenland–Iceland Seas. In addition to bathymetry, land elevation is also included (Fig. 2). The IBCAO grid is an improvement on other regional bathymetric charts available for the Arctic Ocean. However, it contains notable errors and processing artefacts. In particular, the errors consist of artificial terracing that results from a processing overemphasis of digitized contours, as well as miscalibrated ship track soundings that create visible 'streaks' of erroneous data. In addition, limited spatial resolution (6.25 km^2) permits only large-scale analysis and does not warrant the analysis of many smaller slope features.

The new grid is used in this study to characterize the large-scale morphology of a span of Arctic and other high-latitude continental slopes by measuring slope angle and bathymetric roughness with a raster GIS package. These simple parameters are then compared between recently ice-dominated and ice-free regions, as well as differing glacial sedimentary environments to assess possible links between sedimentary processes and margin form.

Data preparation and analysis

Previous GIS-based studies of the continental slope have used high-resolution multibeam bathymetry to assess such problems as slope

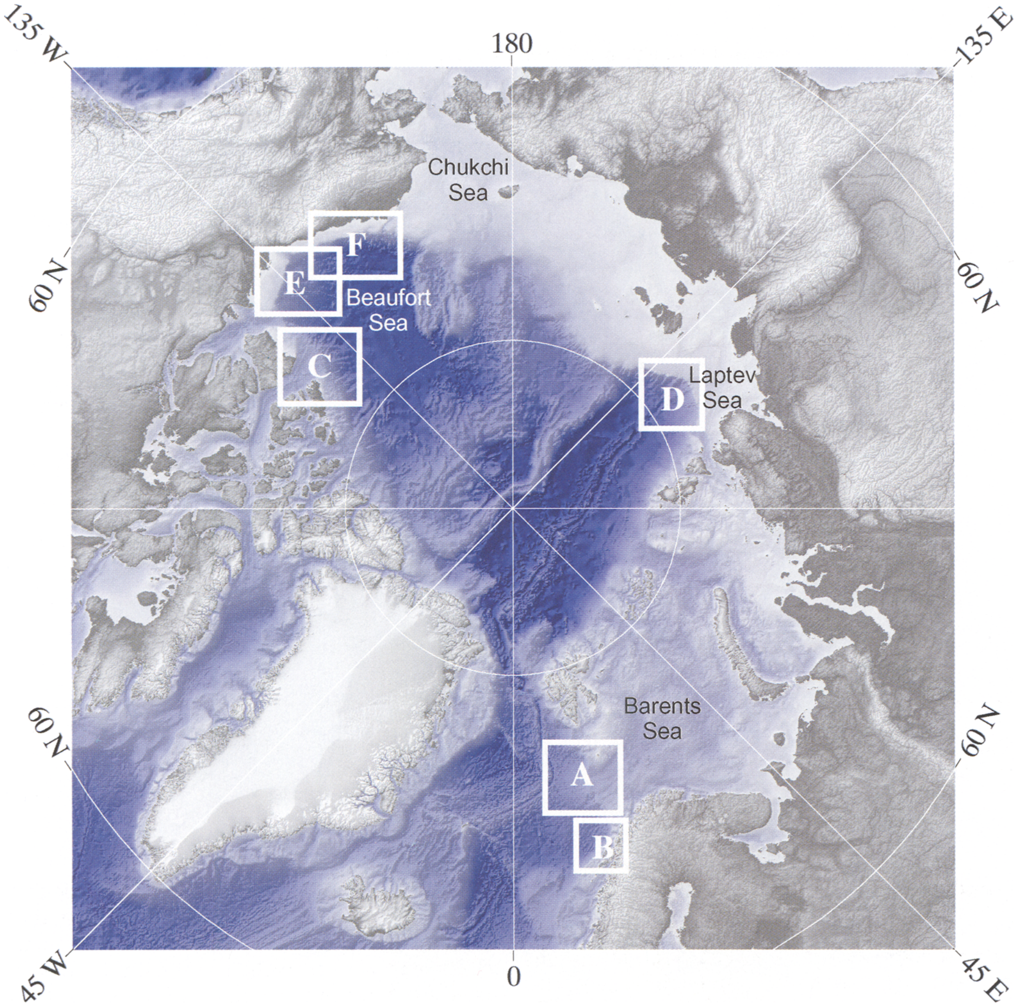

Fig. 2. International Bathymetric Chart of the Arctic Ocean (IBCAO) digital bathymetric model (Jakobsson *et al.* 2000). The six rectangles show the locations of margins discussed in the text and shown in Figure 6.

stability and the geomorphology of mass movements (Lee *et al.* 1999; McAdoo 1999; McAdoo *et al.* 2000). This study attempts to capture a regional perspective on continental slope morphology from data with a much lower spatial resolution. Because of the limited resolution, our morphological analysis is generalized in its treatment of most slope features. For example, only deep-sea features larger than several pixels (50 km^2) can be resolved clearly by the IBCAO data, therefore, large deep-sea canyons may not be clearly defined. Often such large features are present and visible but their dimensions are imprecise. Smaller features, such as slope gullies and rills, are not resolved at all. This aspect of the data limits the quality of spatial analysis that can be performed. By default, the focus of our analysis is on large-scale morphological parameters, particularly general slope gradient and macro roughness. For lower-latitude margins, this type of large-scale, limited-resolution approach has been successful in illustrating the morphological diversity of global continental slopes and its relation to a margin's general sedimentary environment (O'Grady *et al.* 2000).

(a)

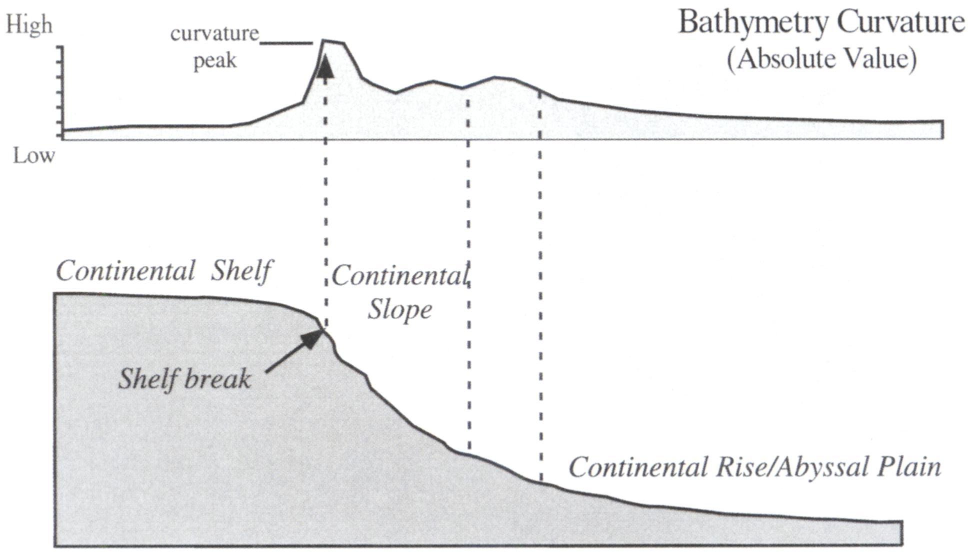

(b)

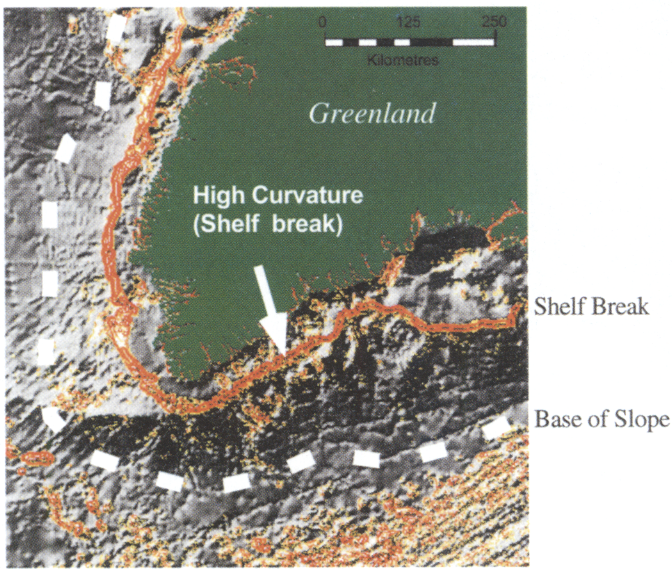

Fig. 3. Definition of the continental slope in terms of bathymetric curvature, or second derivative. (**a**) Relationship between curvature and a hypothetical bathymetric profile. (**b**) An example from the margin of southern Greenland where shelf-break curvature values are much higher than those at the base of the continental slope.

Defining the continental slope

A GIS mask defining the boundaries of the continental slope for the Arctic Ocean was produced to constrain the spatial analysis to the slope. The upper and lower boundaries of the continental slope are defined primarily by bathymetric curvature (the rate of change of sea-floor gradient; Fig. 3a). The upper boundary, the shelf–slope break, is marked as the region just

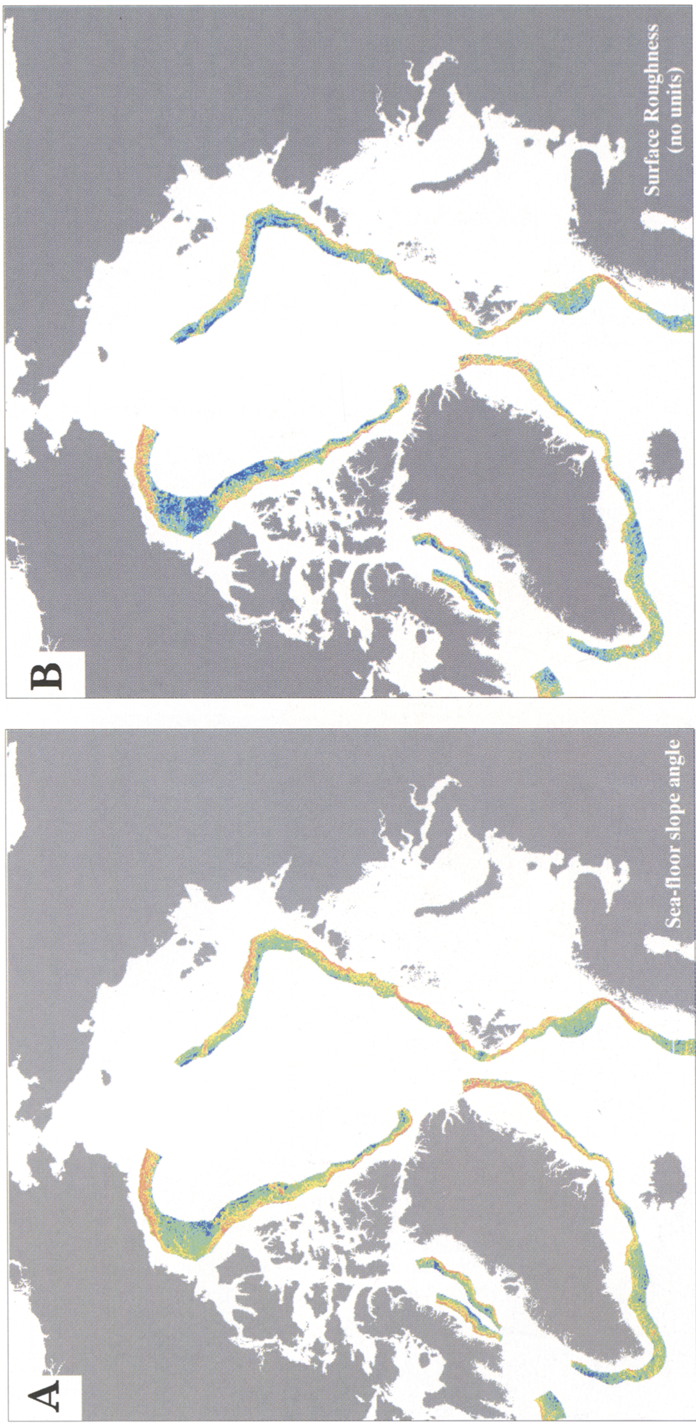

Fig. 4. Results of spatial algorithms on masked slope bathymetry. **(a)** Slope angle for each pixel calculated by averaging the slopes within a 3 × 3 moving window. **(b)** The residual result of a high-pass filter applied to bathymetry. Parameter in **(b)** is used to characterize bathymetric 'roughness' of the continental slope.

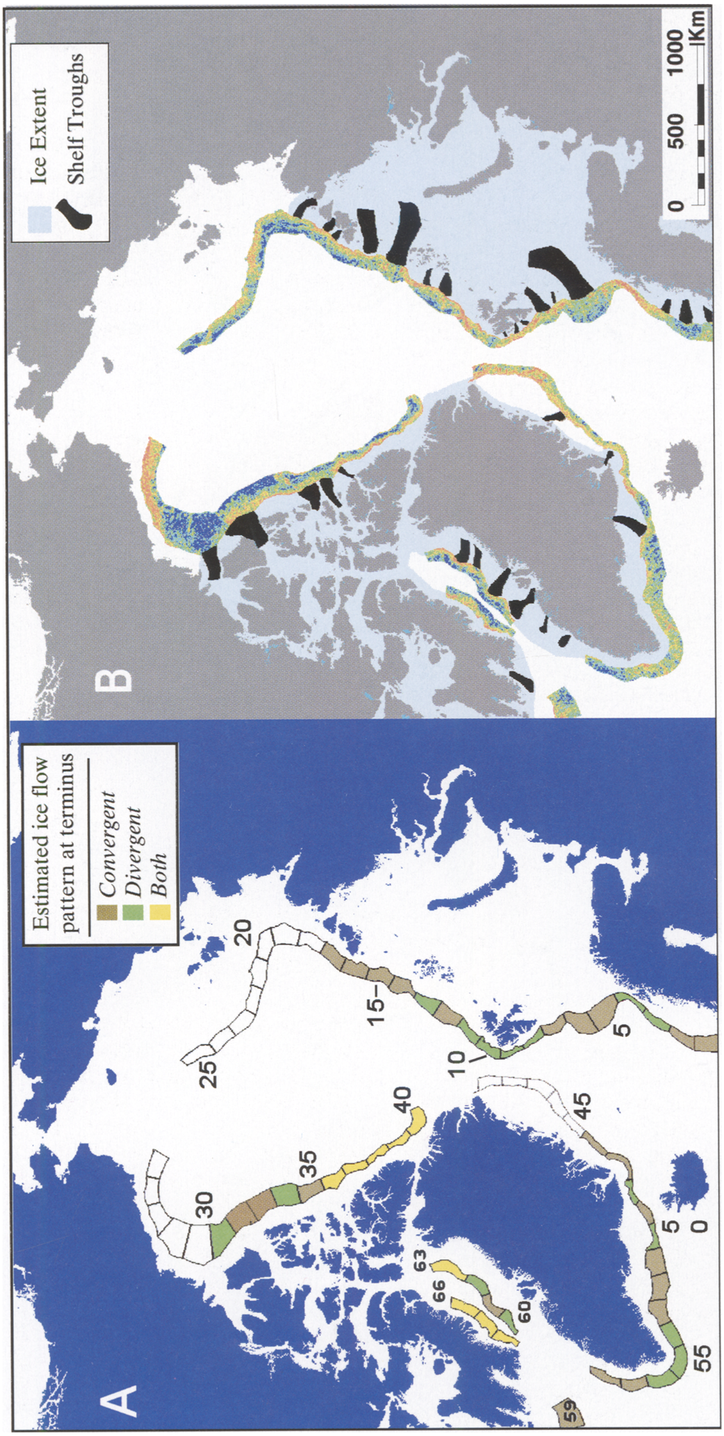

Fig. 5. **(a)** Arbitrary polygons used in the analysis. Numbers correspond to those in Appendix 1. **(b)** Limits of maximum ice extent for the last 130 ka, used in this study. Compiled from several sources described in text.

below the continental shelf with the highest curvature values. The lower boundary is defined as the zone where a significant decrease in slope angle occurs. This boundary is more difficult to define because the changes in slope angle are less dramatic than for the shelf break and thus curvature values are lower and less indicative of its location. The nature of the lower transition is also inconsistent along the margin. A generalized method, such as picking a cut-off slope angle to define the transition from slope to rise (i.e. 1.43° as defined by Heezen 1956) was not used because it is too rigid and not widely applicable to the diverse morphologies in the study. Instead, the base of the slope is defined on a case-by-case basis, using shaded relief, curvature, slope, and general appearance of the surrounding bathymetry as a guide (Fig. 3b). The continental slope mask avoids seamounts and other volcanic or tectonic features. Excluded from the mask are the Chukchi Borderland and the margin of northern Greenland. In addition, the continental slopes of Iceland are left out because of the dominant influence of tectonics on slope morphology.

The slope angle of each pixel was calculated using the average slope of a 3 pixel by 3 pixel scanning window (Fig. 4a). Surface roughness of the bathymetry was analysed by applying a high-pass filter that accentuates high-frequency changes in sea-floor elevation (Fig 4b; Appendix 1). The roughness parameter assists in estimating the presence of slope canyons and down-slope sediment-drainage features. Many smaller canyons are not resolved by the grid, but instead appear in the data as undulating or rough surfaces. We assume that areas with greater density of canyons are likely to have higher surface roughness.

Subdivisional polygons

To simplify the spatial analysis, our span of Arctic continental slopes is divided into 66 polygons, equally spaced at 200 km along margin strike (Fig. 5a). Averages and/or variance statistics within each polygon are used for comparison of slopes and roughness among the different regions. Mean slope angle of a polygon is calculated by averaging the slope of all pixels within the polygon boundaries. Average surface roughness of a polygon is estimated by first calculating the difference between the results of a high-pass filter and the original bathymetric grid. The standard deviation of the residuals for the entire polygon is then calculated. This provides an 'average' roughness parameter to compare between polygons. The arbitrary polygon width of 200 km is used to avoid over-selection of prominent margins and to keep polygon areas relatively equal. The average area of the polygons is 25×10^3 km^2. Spatial statistics are summarized in Appendix 1.

Ice extent

We use previously published studies to define regions of the Arctic that have experienced significant continental-shelf glaciation in the Late Quaternary. Delineating ice extent for this period is difficult, due to existing controversy regarding the Last Glacial Maximum (LGM, *c.* 18 ka) and prior ice advances (Dyke & Prest 1987; England 1998; Grosswald & Hughes 1999; Svendsen *et al.* 1999; Jakobsson *et al.* 1999; Brigham-Grette 2001). However, reasonable confidence exists for many regions of the Arctic (Funder & Hansen 1996; Landvik *et al.* 1998).

Because modern slope morphology is a product of past deposition and erosion as well as recent and modern processes, we chose a span of geological time to focus our study. The time frame considered begins at the last interglacial from isotope substage 5e (*c.* 130 ka) and ends after the LGM. This time interval covers several different ice advances that have brought glacial termini (and river mouths) to the shelf edge, thus influencing slope sedimentation. By encompassing several ice advances, the chosen time frame also allows enough flexibility for diachronous limits of maximum ice extent since glacial ice advance to the shelf edge was episodic and spatially variable. The ice limit shown in Figure 5b is a non-contemporaneous maximum for the Late Quaternary based on several studies (Dyke & Prest 1987; Funder & Hansen 1996; England 1998; Landvik *et al.* 1998; Svendsen *et al.* 1999). For the purpose of our study, we assume that glacial conditions over this time period were important in modifying the shape and character of the continental slope so that their effects are observed in the modern morphology of the margin. This assumption may not be entirely valid since the rates of erosion and deposition are highly variable for the few continental slopes where these parameters have been measured (Faleide *et al.* 1996; Elverhøi *et al.* 1998; Nam & Stein 1999; Andrews 2000). However, generalization of the last glacial cycle provides a baseline from which to analyse process/morphology associations.

Character of ice flow

Using the methods of Syvitski & Praeg (1989) and Syvitski (1993) and maps of Denton &

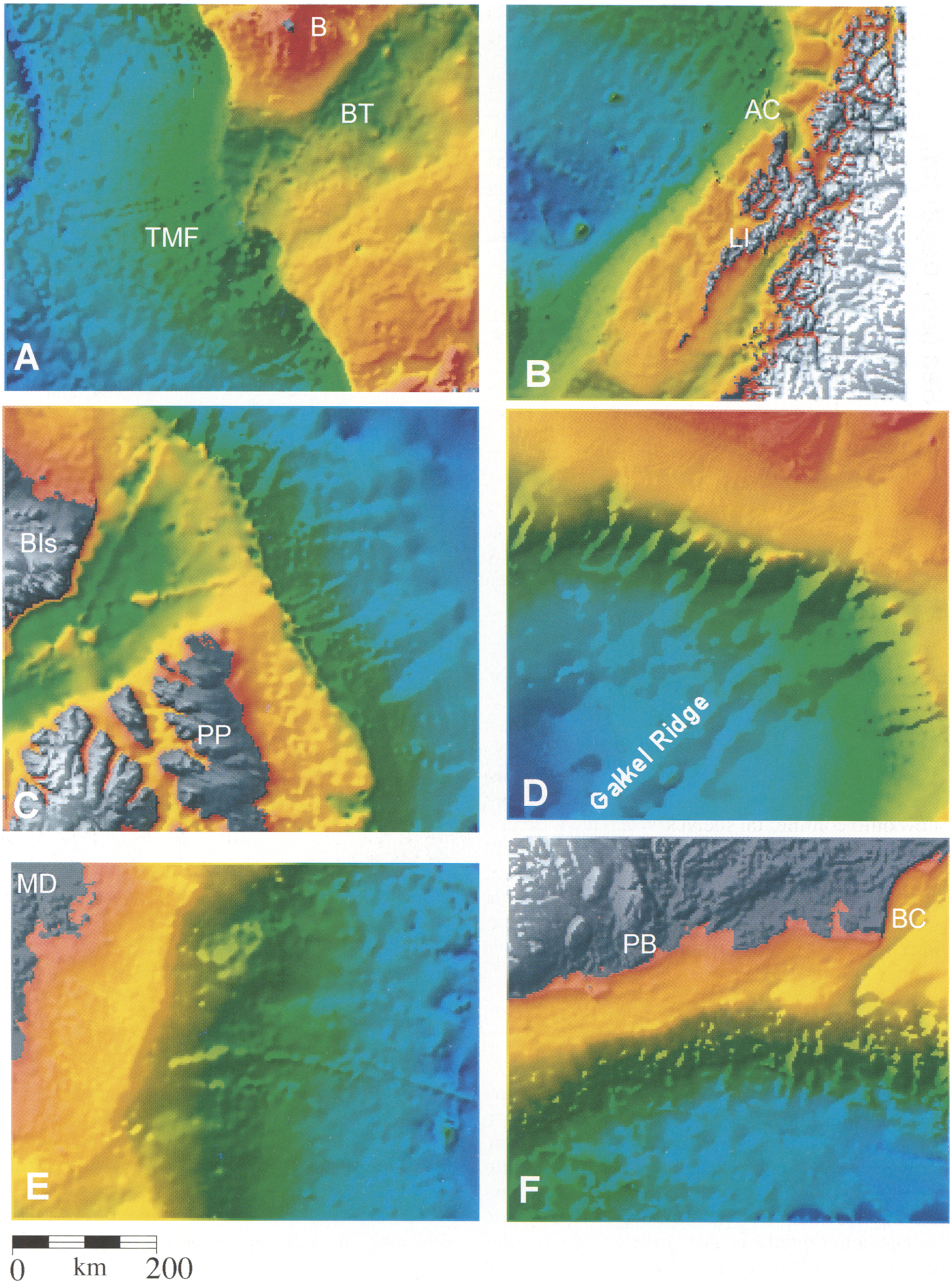

Fig. 6. Six shaded images of continental margins from the IBCAO. In all images red indicates shallow water, blue indicates deeper water. (**a**) Bear Island Fan: B, Bear Island; BT, Bear Island Trough; TMF, trough mouth fan. (**b**) Northern Norway: LI, Lofoten Islands; AC, Andøya Canyon. (**c**) Canadian Archipelago: BIs, Banks Island; PP, Prince Patrick Island. (**d**) Laptev Sea near Lena River. (**e**) Mackenzie Delta Margin: MD, Mackenzie Delta. (**f**) North Slope Alaska: BC, Barrow Canyon; PB, Prudhoe Bay.

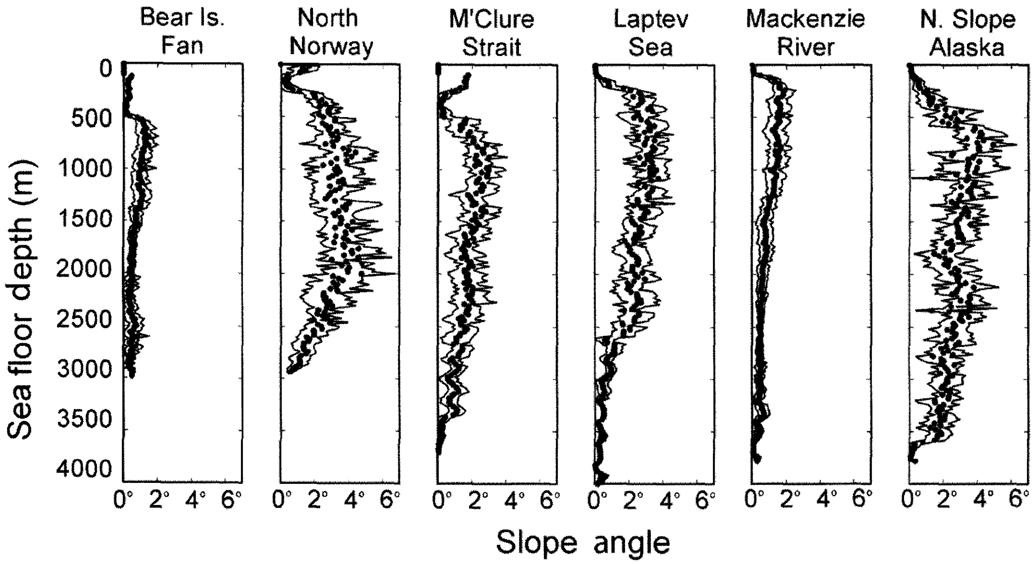

Fig. 7. Slope angle of the sea floor as a function of depth for the margins in Figure 6. Mean slope angle at 20 m depth intervals is represented by a dot and bracketed by lines indicating ± one standard deviation. The sharp increase in slope near the top of each profile represents the shelf–slope break.

Hughes (1981) and Stokes & Clark (2001), we characterize the sedimentary environment at the palaeo-ice sheet terminus in terms of the flow conditions of the glacial ice (Fig. 5a). Ice sheet isopach maps representing the LGM (Syvitski 1993 and references therein) along with modern bathymetry are used to estimate where ice sheet flow onto continental shelves would have experienced either convergent or divergent lines of flow. Glacial troughs on continental shelves provide strong evidence for convergent flow lines (Stokes & Clark 2001), yet convergence is also interpreted for regions that do not have visible troughs. Conversely, inter-trough areas were typically denoted as locations of divergent flow under slow-moving ice conditions. In several instances, the 200 km width of a polygon contains regions of both divergent and convergent palaeo-ice flow. In these cases, an estimate of the dominant flow type is made based on proportions of each flow type. In 9 of 66 polygons we interpret equally convergent and divergent conditions with neither condition having dominance (Figure 5a; Appendix 1).

The convergence or divergence of glacial flow is directly linked to ice velocity and sediment transport to the glacial terminus (Boulton 1990; Dowdeswell & Siegert 1999). In regions of convergence, fast-moving ice delivers relatively greater amounts of sediment in comparison to regions where slow-moving, divergent flow occurs.

Representative Arctic margins

We use six Arctic margins to illustrate various aspects of slope morphology and its relevance to the recent styles of margin sedimentation (Figs 2 & 6): (A) convergent ice flow (ice stream) margin (Bear Island Fan); (B) divergent ice flow (ice-sheet) margin (northern Norway); (C) ice shelf margin (M'Clure Strait); (D) non-glaciated margin with a wide continental shelf (Laptev Sea); (E) non-glaciated, high sediment supply margin (Canadian Beaufort Sea) and (F) non-glaciated, alpine river-dominated margin (North Slope of Alaska). These examples represent a variety of sedimentary environments and exhibit a wide range of morphologies. They also provide a means to evaluate the clarity and quality of the IBCAO bathymetric data used in our analyses (Fig. 6). Plots of sea-floor slope versus sea-floor depth for each locality (Fig. 7) assist in the evaluation of slope morphology. A brief and qualitative summary of each margin is included in Table 1.

Convergent-flow ice-stream margin, Bear Island Fan

Ice streams form as a result of an ice sheet experiencing strongly convergent ice flow. The resultant high flow velocities promote high basal shear stress along with significant concomitant basal sediment transport (Boulton 1990; Alley

Table 1. *Qualitative description of six representative Arctic continental slopes (see Figs 2, 6 & 7)*

Margin	Sedimentary environment	Slope	Shelf width	Shelf break depth	Canyons
Bear Island Fan	Convergent flow ice stream margin,	Gentle	Wide	Deep	Low
Northern Norway	Divergent flow (ice-sheet) margin	Steep	Narrow	Medium	High
M'Clure Strait, Can. Arch.	Ice shelf margin	Medium	Wide*	Deep	High
Laptev Sea	Non-glaciated, large shelf margin	Steep	Very wide	Shallow	High
Beaufort Sea	Non-glaciated, high sediment-supply margin	Gentle	Narrow–medium	Shallow	Low
North Slope of Alaska	Non-glaciated, alpine river-dominated margin	Steep	Narrow–medium	Shallow	High

*Includes M'Clure Strait itself.

et al. 1996). Trough mouth fans, such as the Bear Island Fan (BIF; Fig 6a), are products of high sediment delivery to the shelf edge by ice streams. Sea floor gradients on the BIF are very low, rarely exceeding 1° (Fig. 7; Laberg & Vorren 1996*b*). The fan is composed of successions of mass-flow deposits from repetitive debris flows. The debris flows were generated during times of glacial advance when an ice stream delivered large quantities of basal debris to the shelf edge (e.g. Alley *et al.* 1996; Dowdeswell & Siegert 1999; Dimakis *et al.* 2000). Often the episodic advances remain at the shelf edge only briefly, for a few thousand years at a time (Vorren & Laberg 1997). The persistent recurrence of shelf trough erosion and slope depositional processes, during repeated glaciations, has contributed to the immense size of the Bear Island Fan.

The IBCAO image of the fan shows a smooth and gently sloping feature with few to no visible evidence for canyons or other channels (Fig. 6a). One prominent feature is the large slide scar that breached the shelf break in the late Pleistocene (Laberg & Vorren 1993).

Divergent-flow (ice-sheet) margin, Northern Norway

Slow-flowing areas of ice sheets are often associated with divergent flow line gradients, little basal erosion, and low sediment supply to the continental slope (Boulton 1990). The continental margin of northern Norway (Figs 2 & 6b) is an example of a recently-glaciated shelf located adjacent to a steep continental slope with numerous canyons (Taylor *et al.* 2000). The glaciers in this region during the LGM were not as significant producers and transporters of sediment as the shelf-eroding ice streams to the north and south (Dowdeswell & Siegert 1999; Stokes & Clark 2001). Instead, this portion of the Scandinavian Ice Sheet was slow moving (divergent ice flow) and probably relatively clean, transporting little sediment to the slope, even though the terminus probably reached the shelf edge (Dowdeswell *et al.* 1996). The Lofoten Islands may also have acted as a barrier to ice and sediment flux to the shelf edge (Laberg *et al.* 1999). As a consequence, sediment deposition was not able to fill in the canyons or prograde the slope and contourite deposition was prominent (Laberg *et al.* 1999). In addition to sedimentary processes, the steepness of the margin and perhaps initiation of the canyons themselves may have been influenced by uplift of the region in the Cenozoic (Henriksen & Vorren 1996).

The IBCAO data are not able to show individual canyons aside from perhaps Andøya Canyon (cf. Laberg *et al.* 2000). Several other canyons to the south of Andøya Canyon that have been observed with independent, higher-resolution data (Taylor *et al.* 2000), are represented in the IBCAO only as an irregular sea floor (Fig. 6b).

Ice-shelf margin, M'Clure Strait, Canadian Archipelago

An ice shelf is the seaward margin of an ice sheet where a significant portion of the terminus is not grounded but floating above the sea floor. As such, ice shelves are unable to transport sediment as a subglacial deforming layer to their seaward edge, rather only to their grounding line. Ice shelves are restricted to high-polar environments (Anderson *et al.* 1991), where ablation occurs from iceberg calving and basal melting. Ice shelves often require high ice velocities, and sometimes the aid of geometric constraints such as valley walls and pinning points to grow and survive (Syvitski 1993). Although the palaeo-distribution of ice shelves has been highly controversial (Syvitski 1993), as is the ice extent in the LGM in the NW Canadian Archipelago (England 1998), M'Clure Strait may have been occupied by an ice shelf (Dyke & Prest 1987) (Figs 2, 6c). Bathymetry within the strait and on the adjacent shelf shows a possible glacial trough and suggests the presence of a pre-LGM ice stream (e.g. Denton & Hughes 1981). The continental slope seaward of M'Clure Strait exhibits large canyon-like features in the IBCAO, although no direct studies confirm this.

Non-glaciated large shelf margins, Laptev Sea

The Laptev Sea shelf extends 300 km from the coast to the shelf-slope break and was not glaciated during the LGM (Svendsen *et al.* 1999; Fig. 6d). During that time, the Laptev Sea shelf was exposed due to the lowered sea level (*c.* 120 m; Fairbanks 1989), and several studies reveal that there was no large LGM ice sheet in this area (e.g. Dunayev & Pavlidis 1988; Hahne & Melles 1997; Kleiber & Niessen 1999; Svendsen *et al.* 1999). Instead, the surrounding land masses of the Laptev Sea contained local glaciers (Arkhipov *et al.* 1986; Velichko *et al.* 1997; Kleiber & Niessen 1999). During the LGM, lowstand river runoff continued through four valleys on the exposed Laptev Sea shelf (Kleiber & Niessen 2000). Late Weichselian shelf sediments are generally very fine grained (up to 70% clay), and sand and gravel are almost absent indicating that sediment transport by icebergs was of minor importance (Müller 1999).

The modern environment of the Laptev Sea is influenced strongly by a large volume of fresh water delivered by five major river systems (Khatanga, Anabar, Olenek, Lena, Yana). The Lena River alone contributes approximately 520 km^3 a^{-1} of fresh water (Aargaard & Carmack 1989). Riverine sediment discharge into the Laptev Sea contributes 24 Mt a^{-1}, of which more than 70% comes from the Lena River (Rachold *et al.* 2000; Gordeev *et al.* 1996). Sediment input by coastal erosion contributes another 30 to 58 Mt a^{-1} (Rachold *et al.* 2000; Müller-Lupp *et al.* 2000). Most of the modern sediment deposition is confined to the inner shelf. The depositional history of the outer Laptev Sea shelf during the Holocene is, therefore, coupled strongly with the postglacial sea-level rise (Müller-Lupp *et al.* 2000).

The continental slope of much of the Laptev Sea appears to be dissected with canyons that are very large and regularly spaced. It is unknown whether these canyons relate to sediment erosion by turbidity currents during periods of low sea-level stands, or whether they relate to density currents created by seasonal sea-ice formation. The loss of buoyancy of the shelf waters caused by convective cooling and brine input due to sea-ice formation may lead to convective downward motion on the shelves and the draining of shelf water via density plumes into the central Arctic Ocean basin (Stein 1998).

Non-glaciated, high sediment-supply margin, Canadian Beaufort Sea

The continental slope seaward of the Mackenzie Delta is broad and relatively featureless as imaged by the IBCAO data (Figs 2 & 6e). A weak sign of a modern canyon in the data is more likely an erroneous ship track since seismic data in the region provide no such evidence (Dixon *et al.* 1992). Unlike the Laptev margin, the Beaufort Sea shelf is small, less than 100 km wide, and at least some fraction of sediment discharged by the modern Mackenzie River bypasses the shelf and is deposited on the continental slope (Giovando & Herlinveaux 1981). The Laurentide Ice Sheet has periodically covered the Mackenzie Delta, sometimes affecting the direction of the Mackenzie drainage (Duk-Rodkin & Hughes 1994). However, there is little evidence that the ice sheet reached the shelf–slope break during the LGM (Lemmen *et al.* 1994). The Canadian Beaufort Sea receives a riverine sediment discharge of 64 Mt a^{-1}, mainly from the Mackenzie River, which is the largest single source of sediment delivery in the Arctic (Rachold *et al.* 2000). The low-angle and uniform swath of continental slope is comparable to that of the Bear Island Fan (Fig. 7). In both cases, high sediment flux is a common factor.

Non-glaciated, alpine river-dominated margin, North Slope of Alaska

This section of continental slope is noticeably irregular in texture (Figs 2 & 6f). The large

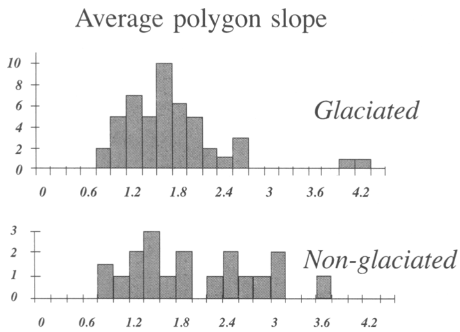

	Mean	Stan. Dev.	N
Glaciated	1.58	0.67	48
Non-glaciated	1.87	0.85	18

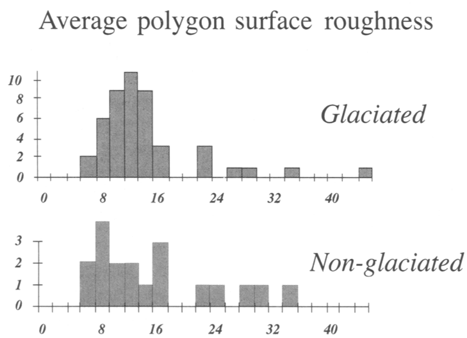

	Mean	Stan. Dev.	N
Glaciated	12.9	7.07	48
Non-glaciated	13.8	8.66	18

Fig. 8. Histograms and statistics of polygon slope angle and roughness for glaciated and non-glaciated polygons.

Barrow Canyon, which incises the shelf on its way to the continental slope, was carved by drainage of the Chukchi Sea during Quaternary sea-level fall (Garrison & Becker 1976). The shelf of the Alaskan North Slope is commonly interpreted as having been ice-free during the LGM (Dyke & Prest 1987), although extensive ice cover has been proposed (Hughes & Hughes 1994).

The Barrow Canyon is resolved adequately by the IBCAO but no canyons to the east are resolved. The rugged surface texture probably reflects massive slope failure caused by decomposing gas hydrates (Kayen & Lee 1991). In seismic reflection images, the margin is characterized by large, deep-seated faults that have contributed to slope failure at the sea floor (Grantz *et al.* 1990).

The North Slope margin of Alaska receives direct sediment input from high-yield alpine rivers, but the local drainage area is small by Siberian and Mackenzie scales, and this limits the sediment delivery to the margin. The largest river is the Colville River which delivers 6 Mt a^{-1} (Milliman & Syvitski 1992), but even that system does not discharge its sediment across the continental shelf (Barnes & Reimnitz 1974; Walker 1974). Much of the sediment on the continental slope is believed to have been delivered during periods of low sea level.

Pan-Arctic comparison of slope morphology

The results of the comparative analyses of Arctic slopes are discussed by addressing two hypotheses:

Hypothesis 1: Continental slope morphology for high-latitude margins is related to different methods of sediment delivery to the slope.

Of the 66 polygons, 48 are adjacent to shelves that were glaciated in the Late Quaternary, with the remaining 18 being predominantly ice-free (Appendix 1). Average slope angle of the continental slope for glaciated margins ranges from 0.61° to 4.0° with a mean of 1.58°. For the non-glaciated margins the range is from 0.75° to 3.5° with a mean of 1.87° (Fig. 8). Results of a Kolmogorov–Smirnov (K–S) test, a non-parametric statistical test that determines whether two datasets differ significantly (Davis 1986), suggests that values of slope angle and roughness between glaciated and non-glaciated polygons are statistically distinct. In the case of the two distributions in Figure 8, the K–S statistic is 0.260 and the two-tailed critical K–S value at 95% confidence is 0.247. The null hypothesis, which states that the two distributions are the same, is subsequently rejected. This result reinforces an intuitive concept that slope transport driven by glacial activity is different from that controlled by fluvial sources. However, in both environments the range in slope and slope roughness is large and their ranges overlap significantly. The range of slopes shown in this analysis of pan-Arctic margins, both glacial and otherwise, generally falls within the range of mean slopes calculated for most low-latitude, river-dominated margins (O'Grady *et al.* 2000).

A closer look at glacial environments shows

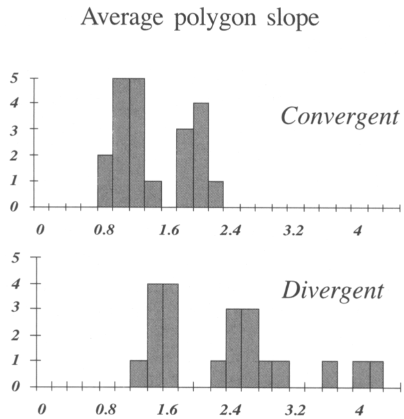

	Mean	Stan. Dev.	N
Convergent	1.29	0.46	21
Divergent	2.17	0.90	21

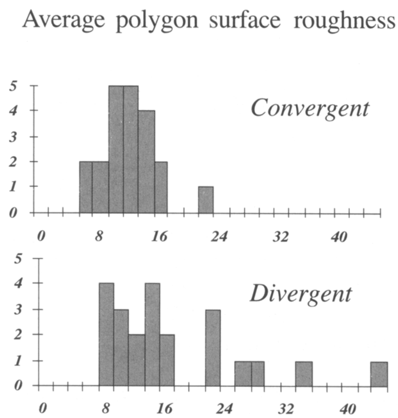

	Mean	Stan. Dev.	N
Convergent	10.8	3.7	21
Divergent	16.5	9.4	21

Fig. 9. Histograms of slope angle and roughness for polygons adjacent to convergent and divergent ice margins.

that margins that experienced a predominance of convergent ice flow have gentler and less rough continental slopes when compared to margins that have experienced predominantly divergent ice flow conditions (Fig. 9). Many of the divergent margins are quite steep. Divergent ice margins are likely to have received less sediment input during the previous glacial cycles leading to a dominance of erosional processes on the continental slope and steeper slope angles (O'Grady *et al.* 2000; Taylor *et al.* 2000). A K–S test between these two distributions also suggests a statistical distinction.

Given our generalized subdivisions, we can safely accept Hypothesis 1 as reasonable. However, we cannot discern the influence of specific sedimentary processes on the shape of the continental slope.

Hypothesis 2: The continental slope gradient of trough-mouth fans is a direct function of long term sediment delivery from fast-flowing ice streams.

Glacial troughs are assumed to indicate erosion of the continental shelf and sediment transport to the slope by fast-moving ice streams (Alley 1996; Ottesen *et al.* 2002). At the glacier terminus (commonly the shelf–slope break) deposition occurs rapidly, leading to sea-floor failure, debris-flow accumulation, and fan development (Vorren *et al.* 1998; Kuvaas & Kristoffersen 1991). Investigated trough-mouth fans tend to show similar morphologies, having low-angle profiles and few canyons (Faleide *et al.* 1996), suggesting that a distinction from the morphology of other margins is likely. We find that trough-fed polygons exhibit a range in mean slope from 0.82° to 2.57° with a mean of 1.59°.

Twenty-seven glacial trough features have been identified on the continental shelf in our analysis of the IBCAO. These features correspond to 20 of the glaciated polygons (Fig. 5b; Appendix 1). All of these troughs are assumed to be at least partially modified by fast-flowing ice. Glacially carved troughs are distinguished from other fluvial-derived channels by their dimensions and morphology. Many small troughs are overlooked because of the spatial resolution of the bathymetric data. In addition, ice-stream marginal width is likely to be smaller than the polygon width of 200 km. Therefore the mean slope gradient of a polygon includes the fans and, if the fan is small, portions of the adjacent continental slope as well.

To help explain the variation in slope gradient of trough-fed polygons, the average distance of a polygon's shelf edge border to the nearest coastline was calculated. This parameter is essentially a rough calculation of the width of the continental shelf adjacent to each polygon (Appendix 1). We suggest that shelf width may also be considered a proxy for the amount of sediment delivered to the slope by an adjacent ice stream. Anderson (2001) demonstrates that

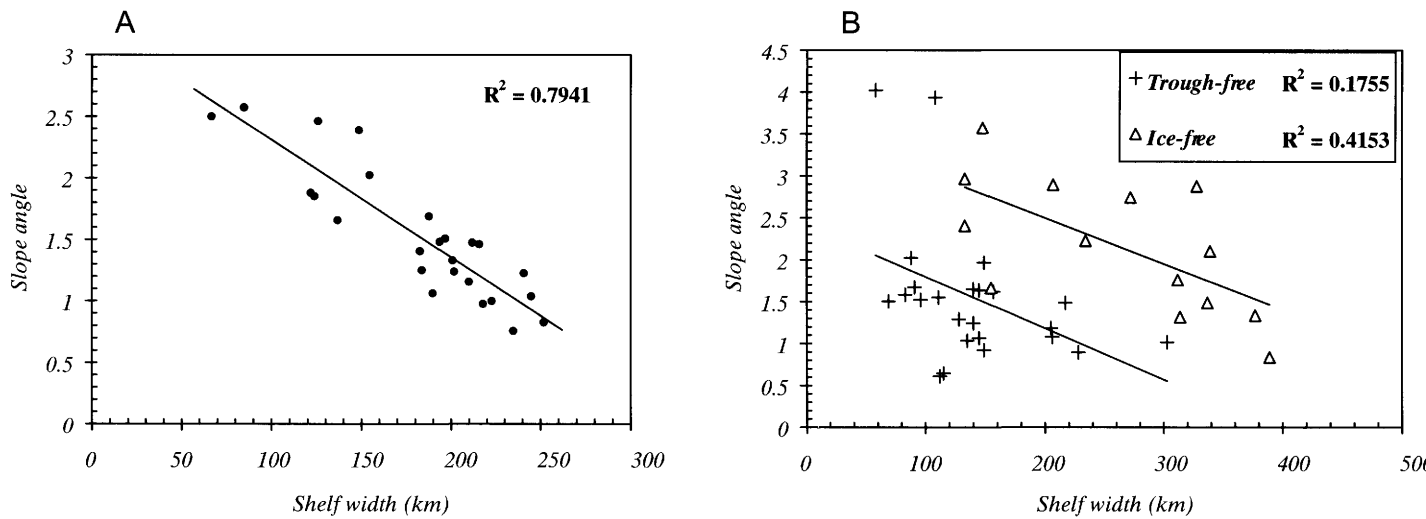

Fig. 10. Scatter plots of approximate shelf width v. mean polygon slope angle. (**a**) Only trough-fed polygons are represented. (**b**) Polygons without adjacent troughs, both glaciated and ice-free groups.

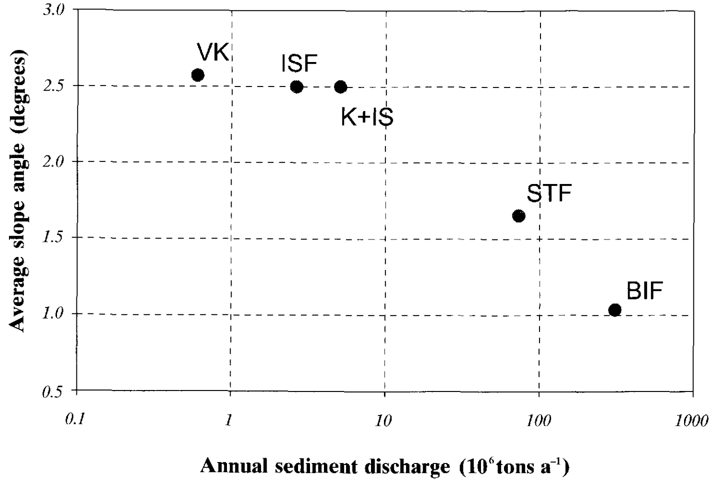

Fig. 11. Sediment discharge data for several glacial margins and trough-mouth fans (Elverhøi *et al.* 1998) plotted against average slope gradient of the adjacent polygon. Three measurements are from fans: BIF, Bear Island Fan; Polygon 5–6. STF, Storfjorden Fan; Polygon 7. ISF, Isforden Fan; Polygon 9. Two measurements are from fjords: K+IS, Kongsforden and Isforden; Polygon 9. VK, Van Keulenfjorden; Polygon 8.

continental shelf sediments are more easily eroded by fast-moving ice than is crystalline bedrock, suggesting that a wide swath of shelf is apt to contribute more to an ice-stream's sediment load than hinterland erosion.

A simple plot of mean slope angle versus approximate shelf width for trough-fed margins (Fig. 10a) shows a roughly linear relationship between the two parameters. This relationship is not exhibited by trough-absent, or ice-free margins (Fig. 10b). Near one end of the linear correlation is the Bear Island Fan which has a very large shelf width (245 km) and a low average slope (1.04°). At the other end (2.6°) is the fan adjacent to Kongsfjorden in western Spitsbergen (Landvik *et al.* 1998).

Estimates of sediment flux to a few trough mouth fans presented in the literature support this finding (Elverhøi *et al.* 1998). The flux estimates come from both volumetric estimates on the fans themselves over portions of the Cenozoic or in the adjacent fjords during the Holocene (Elverhøi *et al.* 1998). Those fans with the highest estimates of sediment input have most gentle gradients with a systematic trend towards steeper slopes and waning supply (Fig. 11). These results suggest the acceptance of Hypothesis 2.

Model of fan geomorphic development

The association between slope angle and sediment input to trough-mouth fans may be related to the stratigraphic development of a fan. As a glacial trough develops by erosion and sediment delivery across the shelf, initial accumulation of debris on the continental slope by mass flow occurs mostly at the base of the steep bedrock-controlled continental slope (Fig. 12). Deposition at the base of a steep slope is typical for subaqueous debris flows, observed in experiments (Mohrig *et al.* 1999), field data (Hampton *et al.* 1996), and numerical models (O'Grady & Syvitski 2001). A feedback occurs whereby base-of-slope deposition builds up the lower slope and reduces its gradient, in turn inducing more deposition on the slope. The consequence is that the slope angle of a developing fan becomes more gentle and more prone to on-slope deposition by mass flows through time and less prone to bypass of flows to the basin floor. However, many large slides have occurred on very shallow slopes (Hampton *et al.* 1996).

A geomorphically 'mature' fan is one that has built up the slope to the point where subsequent deposition perpetuates a similar low-gradient morphology (e.g. the Bear Island Fan). Maturity is likely to be a function of time and/or the rate of sediment delivery to the fan. Fans with high gradients (about 4°) are closer to a geomorphically 'young' developmental stage because they have received less sediment over their history than 'mature', low gradient fans. The terms 'youthful' or 'mature' refer to stages of geomorphic development and do not imply any

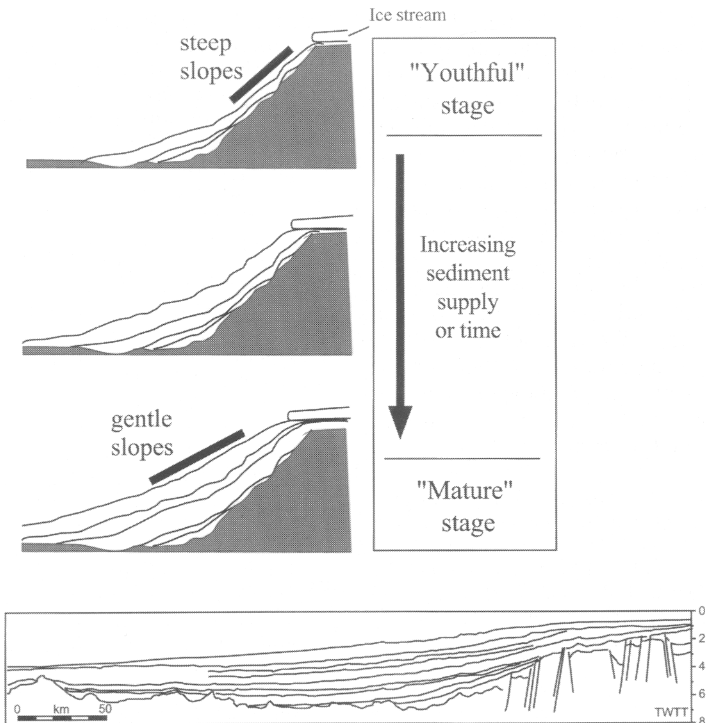

Fig. 12. The relationship between slope angle of trough-mouth fans and the stratigraphic development of a fan. Below is an interpreted multi-channel seismic record of the Bear Island Fan (from Faleide *et al.* 1996). Stratigraphy spans more than 50 Ma; however, most deposition occurred over the last 2.5 Ma with the onset of widespread glaciation.

respective age. For example, the margins of northern Svalbard were recipients of glacial sediment approximately 200 000 years before the Bear Island Fan (Solheim *et al.* 1998). However, the Bear Island Fan has matured faster due to the high rate of sediment influx.

Examples from multi-channel seismic reflection data for Bear Island Fan (Faleide *et al.* 1996) suggest that the proposed evolution model might be relevant for this margin. Sediments at the base of the stratigraphic section, although probably not glacial in origin (Vorren *et al.* 1991; Solheim *et al.* 1998), have accumulated initially at what seems to be the base of the continent–ocean crust boundary slope. Over time, the continental slope has built outward and upward, decreasing its overall gradient (Fig. 12). Debris flow deposition of the last glacial advance is entirely on the slope and is fairly uniformly distributed (Vorren *et al.* 1998). This latest pattern of accumulation has lead to a perpetuation of surface morphology as observed in the repetition of sub-parallel reflections in shallow seismic reflection data (Laberg & Vorren 1996*b*).

Conclusions

The method of sediment delivery to the shelf edge and continental slope appears to play an important role in determining the basic shape and surface morphology of the continental slope. The means of sediment delivery influences the rate and patterns of sediment accumulation on the slope, the types of sediment dispersal mechanisms that are present (e.g. buoyant plumes, icebergs, basal transport), and ultimately the origin of down-slope processes such as slope failures, debris flows, slumps, slides, and turbidity currents. Though the actual sculpting of the sea floor is carried out by these specific processes, the characteristics of sediment delivery (its rate, amount, and location) govern their distribution and activity.

In this study, we have subdivided delivery mechanisms into fluvial (ice-free), convergent ice termini, and divergent ice termini. With simple statistics and morphological analyses we show that margins fed by probable fluvial sources are steeper and exhibit greater surface roughness than those fed from glacial sources. We observe that divergent ice termini associate with steeper and rougher slopes than convergent termini. Glacial trough-mouth fans show a wider range of mean slope angle than expected from previous studies. This range in slope is linked closely with the width of the adjacent continental shelf, and the rate of sediment discharge to the slope. We suggest that the range in the mean slope angle for modern fans may be related to a fan's stage of geomorphic development with respect to the amount of sediment delivered to the margin over its history.

Research support by the Office of Naval Research STRATAFORM project under the leadership of J. Kravitz and C. Nittrouer. An earlier version of the manuscript was greatly improved through the comments of reviewers T. Vorren, A. Elverhøi, and J. A. Dowdeswell. Thanks to S. Principato and W. Manley for helpful insight and suggestions.

References

AAGAARD, K. & CARMACK, E. C. 1989. The role of sea ice and other fresh water in the Arctic Circulation. *Journal of Geophysical Research*, **94**, 485–498.

ADAMS, E. W. & SCHLAGER, W. 2000. Basic types of submarine slope curvature. *Journal of Sedimentary Research*, **70**, 814–828.

ALLEY, R. B., ANANDAKRISHNAN, S. & CUFFEY, K. M. 1996. Subglacial sediment transport and ice-stream behavior. *Antarctic Journal of the United States*, **31**, 81–82.

ANDERSON, J. B. 2001. Geomorphic and sedimentologic records of grounded ice sheets and paleo-ice streams. *Glacier-influenced sedimentation on high-latitude continental margins; a meeting of the Marine Studies Group of the Geological Society, Programme and Abstracts*, 4.

ANDERSON, J. B., KENNEDY, D. S., SMITH, M. J. & DOMACK, E. W. 1991. Sedimentary facies associated with Antarctica's floating ice masses. *In:* ANDERSON J. B. & ASHLEY, G. M. (eds) *Glacial marine sedimentation; paleoclimatic significance*. Geological Society of America, Special Publications, **261**, 1–25.

ANDREWS, J. T. 2000. Explained and unexplained spatial and temporal variability in rates of marine sediment accumulation along the northeast margin of the Laurentide ice sheet < or = 14 Ka. *Journal of Sedimentary Research*, **70**, 782–787.

ARKHIPOV, S. A., BESPALY, V. G., FAUSTOVA, M. A., GLUSHKOVA, O., ISAYEVA, L. L. & VELICHKO, A. A. 1986. Ice sheet reconstructions. *Quaternary Science Reviews*, **5**, 475–483.

BARNES, P. W. & REIMNITZ, E. 1974. Sedimentary processes on arctic shelves off the northern coast of Alaska. *In:* REED, J. C. & SATER, J. E. (eds) *The coast and shelf of the Beaufort Sea*. Arctic Institute of North America, Arlington, 439–476.

BOULTON, G. S. 1990. Sedimentary and sea level changes during glacial cycles and their control on glacimarine facies architecture. *In*: DOWDESWELL, J. A. & SCOURSE, J. D. (eds) *Glacimarine environments: processes and sediments*. Geological Society, London, Special Publications, **53**, 15–52.

BRIGHAM-GRETTE, J. 2001. New perspectives on Beringian Quaternary paleogeography, stratigraphy, and glacial history. *Quaternary Science Reviews*, **20**, 15–24.

DAVIS, J. C. 1986. *Statistics and data analysis in Geology*. Wiley, New York.

DENTON, G. H. & HUGHES, T. J. 1981. The Arctic Ice Sheet: An outrageous hypothesis. *In:* DENTON, G. H. & HUGHES, T. J. (eds) *The last great ice sheets*. Wiley, New York.

DIMAKIS, P., ELVERHØI, A., HOEG, K., SOLHEIM, A., HARBITZ, C., LABERG, J. S., VORREN, T. O. & MARR, J. 2000. Submarine slope stability on high-latitude glaciated Svalbard-Barents Sea Margin. *Marine Geology*, **162**, 303–316.

DIXON, J., DIETRICH, J., SNOWDON, L., MORRELL, G. & MCNEIL, D. H. 1992. Geology and petroleum potential of Upper Cretaceous and Tertiary strata, Beaufort-Mackenzie area, Northwest Canada. *Bulletin of American Association of Petroleum Geologists*, **76**, 927–947.

DOWDESWELL, J. A. & SIEGERT, M. J. 1999. Ice-sheet numerical modeling and marine geophysical measurements of glacier-derived sedimentation on the Eurasian Arctic continental margins. *Bulletin of the Geological Society of America*, **111**, 1080–1097.

DOWDESWELL, J. A., KENYON, N. H., ELVERHØI, A., LABERG, J. S., HOLLENDER, F. J., MIENERT, J. & SIEGERT, M. J. 1996. Large-scale sedimentation on the glacier-influenced polar North Atlantic margins; long-range side-scan sonar evidence. *Geophysical Research Letters*, **23**, 3535–3538.

DOWDESWELL, J. A., ELVERHØI, A. & SPEILHAGEN, R. 1998. Glacimarine sedimentary processes and facies on the Polar North Atlantic margins. *Quaternary Science Reviews*, **17**, 243–272.

DUK-RODKIN, A. & HUGHES, O. L. 1994. Tertiary-Quaternary drainage of the pre-glacial Mackenzie Basin. *Quaternary International*, **22–23**, 221–241.

DUNAYEV, N. N. & PAVLIDIS, J. A. 1988. A model of the Late Pleistocene glaciation of Eurasiatic Arctic Shelf. *In:* KOTLYAKOV, V. M. & SOKOLOV, V. E. (eds) *Arctic research: advances and prospects 2*. Proceedings of the Conference of Arctic and Nordic Countries on Coordination of Research in the Arctic. Academy of Science of the USSR, 70–72.

DYKE, A. S. & PREST, V. K. 1987. Late Wisconsinan and Holocene history of the Laurentide ice sheet. *Geographie Physique et Quaternaire*, **61**, 237–263.

ELVERHØI, A., HOOKE, R. L. & SOLHEIM, A. 1998. Late Cenozoic erosion and sediment yield from the Svalbard-Barents Sea region; implications for understanding erosion of glacierized basins. *Quaternary Science Reviews*, **17**, 209–241.

ENGLAND, J. 1998. Support for the Innuitian ice sheet in the Canadian High Arctic during the last glacial maximum. *Journal of Quaternary Science*, **13**, 275–280.

FAIRBANKS, R. G. 1989. A 17,000-year glacio-eustatic sea level record: influence of glacial melting rates on the Younger Dryas event and deep-ocean circulation. *Nature*, **342**, 637–642.

FALEIDE, J. I., SOLHEIM, A., FIEDLER, A., HJELSTUEN, B. O., ANDERSEN, E. S. & VANNESTE, K. 1996. Late Cenozoic evolution of the western Barents Sea-Svalbard continental margin. *Global and Planetary Change*, **12**, 53–74.

FUNDER S. & HANSEN, L. 1996. The Greenland ice sheet; a model for its culmination and decay during and after the last glacial maximum. *Bulletin of the Geological Society of Denmark*, **42**, 137–152.

GARRISON, G. R. & BECKER, P. 1976. The Barrow submarine canyon: a drain for the Chukchi Sea. *Journal of Geophysical Research*, **81**, 4445–4453.

GIOVANDO, L. F. & HERLINVEAUX, R. H. 1981. A discussion of factors influencing dispersion of pollutants in the Beaufort Sea. *Pacific Marine Science Report*, **81**, 198 pp.

GORDEEV, V. V., MARTIN, J. M., SIDOROV, I. S. & SIDOROVA, M. V. 1996. A reassessment of the Eurasian River Input of water, sediment, major elements, and nutrients to the Arctic Ocean. *American Journal Science*, **296**, 664–691.

GRANTZ, A., MAY, S. D. & HART, P. E. 1990. Geology of the Arctic continental margin of Alaska. *In:* GRANTZ, A., JOHNSON, L. & SWEENEY, J. F. (eds) *The Arctic Ocean Region*. Geological Society of America, Boulder, 257–288.

GROSSWALD, M. G. & HUGHES, T. J. 1999. The case for an ice shelf in the Pleistocene Arctic Ocean. *Polar Geography*, **23**, 23–54.

HAHNE, J. & MELLES, M. 1997. Late- and post-glacial vegetation and climate history of the south-western Taymyr Peninsula, central Siberia, as revealed by pollen analysis of a core from Lama Lake. *Vegetation History Archaeobotany*, **6**, 1–8.

HAMPTON, M. A., LEE, H. J. & LOCAT, J. 1996. Submarine landslides. *Reviews of Geophysics*, **34**, 33–59.

HEEZEN, B. C. 1956. Outline of north Atlantic deep-sea geomorphology. *Geological Society of America Bulletin*, **67**, 1703–1704.

HENRIKSEN, S. & VORREN, T. O. 1996. Late Cenozoic sedimentation and uplift history on the mid-Norwegian continental shelf. *Global and Planetary Change*, **12**, 171–199.

HESSE, R., KLAUCK, I., KHODABAKHSH, S. & PIPER, D. 1999. Continental slope sedimentation adjacent to an ice margin. III. The upper Labrador Slope. *Marine Geology*, **155**, 249–276.

HUGHES, B. A. & HUGHES, T. J. 1994. Transgressions: rethinking Beringian glaciation. *Palaeogeography, Palaeoclimatology, Palaeoecology*, **110**, 275–294.

JAKOBSSON, M., BACKMAN, J. & KNUTSEN, J. O. 1999. Late Pleistocene ice grounding on the Lomonosov Ridge? *In: European Union of Geosciences conference abstracts*; EUG 10 Journal of Conference Abstracts, **4**, 758.

JAKOBSSON, M., CHERKIS, N., WOODWARD, J., MACNAB, R. & COAKLEY, B. 2000. New grid of Arctic bathymetry aids scientists and mapmakers. *Eos*, Transactions of the American Geophysical Union, **81**, 89, 93, 96.

KAYEN, R. E. & LEE, H. J. 1991. Pleistocene slope instability of gas hydrate-laden sediment on the Beaufort Sea margin. *Marine Geotechnology*, **10**, 125–141.

KLEIBER, H. P. & NIESSEN, F. 1999. Late Pleistocene paleoriver channels on the Laptev Sea shelf: implications from sub-bottom profiling. *In:* KASSENS, H., BAUCH, H., DMITRENKO, I., EICKEN, H., HUBBERTEN, H. W., MELLES, M., THIEDE, J. & TIMOKHOV, L. (eds) *Land-ocean systems in the Siberian Arctic: dynamics and history*. Springer, Berlin-Heidelberg-New York, 657–666.

KLEIBER, H. P. & NIESSEN, F. 2000. Variations of continental discharge pattern in space and time: Implications from the Laptev Sea continental margin, Arctic Siberia. *International Journal of Earth Science*, **89**, 605–616.

KUVAAS, B. & KRISTOFFERSEN, Y. 1991. The Crary Fan; a trough-mouth fan on the Weddell Sea continental margin, Antarctica. *Marine Geology*, **97**, 345–362.

LABERG, J. S. & VORREN, T. O. 1993. A late Pleistocene submarine slide on the Bear Island trough mouth fan. *Geo-Marine Letters*, **13**, 227–234.

LABERG, J. S. & VORREN, T. O. 1996*a*. The glacier-fed fan at the mouth of Storfjorden trough, western Barents Sea: a comparative study. *Geologische Rundschau*, **85**, 338–349.

LABERG, J. S. & VORREN, T. O. 1996*b*. The Middle and Late Pleistocene evolution of the Bear Island Trough Mouth Fan. *Global and Planetary Change*, **12**, 309–330.

LABERG, J. S., VORREN, T. O. & KNUTSEN, S. M. 1999. The Lofoten contourite drift off Norway. *Marine Geology*, **159**, 1–6.

LABERG, J. S., VORREN, T. O., DOWDESWELL, J. A., KENYON, N. H. & TAYLOR, J. 2000. The Andøya slide and the Andøya canyon, north-eastern Norwegian–Greenland Sea. *Marine Geology*, **162**, 259–275.

LANDVIK, J. Y., BONDEVIK, S., ELVERHØI, A., FJELD-SKAAR, W., MANGERUD, J., SIEGERT, M. J., SVENDSEN, J. I., & VORREN, T. O. 1998. The last glacial maximum of Svalbard and the Barents Sea area; ice sheet extent and configuration. *Quaternary Science Reviews*, **17**, 43–75.

LEE, H., LOCAT, J., DARTNELL, P., ISRAEL, K. & WONG, F. L. 1999. Regional variability of slope stability; application to the Eel margin, California. *Marine Geology*, **154**, 305–321.

LEMMEN, D. S., DUK-RODKIN, A. & BEDNARSKI, J. 1994. Late glacial drainage systems along the northwestern margin of the Laurentide Ice Sheet. *Quaternary Science Reviews*, **13**, 805–828.

McAdoo, B. G. 1999. Mapping submarine slope failures, *In:* Wright, D. & Bartlett D. (eds) *Marine and coastal geographic information systems*. Taylor and Francis, London.

McAdoo, B. G., Pratson, L. F. & Orange, D. L. 2000. Submarine landslide geomorphology, US continental slope. *Marine Geology*, **169**, 103–136.

Milliman, J. D. & Syvitski, J. P. M. 1992. Geomorphic/tectonic control of sediment discharge to the ocean: the importance of small mountainous rivers. *Journal of Geology*, **100**, 525–544.

Mohrig, D., Elverhøi, A. & Parker, G. 1999. Experiments on the relative mobility of muddy subaqueous and subaerial debris flows, and their capacity to remobilize antecedent deposits. *Marine Geology*, **154**, 117–129.

Müller, C. 1999. Rekonstruktion der Paläo-Umweltbedingungen am Laptev-See-Kontinentalrand während der letzten beiden Interglazial/Glazial-Zyklen anhand sedimentologischer und mineralogischer Untersuchungen. *Berichte zur Polarforsch*, **328**, 1–146.

Müller-Lupp, T., Bauch, H., Erlenkeuser, H., Hefter, J., Kassens, H. & Thiede, J. 2000. Input of terrestrial organic matter into the Laptev Sea during Holocene: Evidence from stable carbon isotopes. *International Journal of Earth Science*, **89**, 563–568.

Nam, S. I. & Stein, R. 1999. Late Quaternary variations in sediment accumulation rates and their paleoenvironmental implications; a case study from the East Greenland continental margin. *In:* Bruns, P. & Hass, H. C. (eds) *On the determination of sediment accumulation rates*. GeoResearch Forum, **5**, 223–240.

O'Grady, D. B. & Syvitski, J. P. M. 2001. Predicting profile geometry of continental slopes with a multiprocess sedimentation model. *In:* Merriam, D. & Davis, J. (eds) *Geologic modeling and simulation: sedimentary systems*. Kluwer Academic/Plenum, New York, 99–117.

O'Grady, D. B., Syvitski, J. P. M., Pratson, L. F. & Sarg, J. F. 2000. Categorizing the morphologic variability of siliciclastic passive continental margins, *Geology*, **28**, 207–210.

Ottesen, D., Dowdeswell, J. A., Rise, L., Rokoengen, K. & Henriksen, S. 2002. Large-scale morphological evidence for past ice-stream flow on the mid-Norwegian continental margin. *In*: Dowdeswell, J. A. & Ó Cofaigh, C. (eds) *Glacier-Influenced Sedimentation on High-Latitude Continental Margins*. Geological Society, London, Special Publication, **203**, 245–258.

Rachold, V., Grigoryev, M. N., Are, F., Solomon, S., Reimnitz, E., Kassens, H. & Antonov, M. 2000. Coastal erosion vs. riverine sediment discharge in the Arctic shelf seas. *International Journal of Earth Science*, **89**, 450–460.

Solheim, A., Faleide, J. I., Andersen, E. S., Elverhøi, A., Forsberg, C. F., Vanneste, K., Uenzelmann, N. G. & Channell, J. 1998. Late Cenozoic seismic stratigraphy and glacial geological development of the East Greenland and Svalbard–Barents Sea continental margins. *Quaternary Science Reviews*, **17**, 155–184.

Stein, R. 1998. *Arctic paleo-river discharge*. Berichte zur Polarforschung, **279**.

Stokes, C. R. & Clark, C. D. 2001. Palaeo-ice streams. *Quaternary Science Reviews*, **20**, 1437–1457.

Svendsen, J. I., Astakhov, V. I., Bolshiyanov, D. Y., *et al.* 1999. Maximum extent of the Eurasian ice sheets in the Barents and Kara Sea region during the Weichselian. *Boreas*, **28**, 234–242.

Syvitski, J. P. M. 1993. Glacimarine environments in Canada: An overview. *Canadian Journal of Earth Sciences*, **30**, 354–371.

Syvitski, J. P. M. & Praeg, D. B. 1989. Quaternary sedimentation in the St. Lawrence Estuary and adjoining areas: an overview based on high resolution seismo-stratigraphy. *Geographie Physique et Quaternaire*, **43**, 291–310.

Taylor, J., Dowdeswell, J. A. & Kenyon, N. H. 2000. Canyons and late Quaternary sedimentation on the North Norwegian margin. *Marine Geology*, **166**, 1–9.

Velichko, A. A., Zelikson, E. M., Morozova, T. D., Nechaev, V. P., Porozhnyakova, O. M. & Chichagova, O. A. 1997. Paleogeographic conditions in the central Russian Plain during the Atlantic period of the Holocene; evidence from data on fossil soil study. *Transactions of the Russian Academy of Sciences*, **6**, 897–900.

Vorren, T. O. & Laberg, J. S. 1997. Trough mouth fans; palaeoclimate and ice-sheet monitors. *Quaternary Science Reviews*, **16**, 865–881.

Vorren, T. O., Richardsen, G., Knutsen, S. M. & Henriksen, E. 1991. Cenozoic erosion and sedimentation in the western Barents Sea. *Marine and Petroleum Geology*, **8**, 317–340.

Vorren, T. O., Laberg, J. S., Blaume, F., Dowdeswell, J. A., Kenyon, N. H., Mienert, J., Rumohr, J. & Werner, F. 1998. The Norwegian–Greenland Sea continental margins: morphology and Late Quaternary sedimentary processes and environment. *Quaternary Science Reviews*, **17**, 273–302.

Walker, H. J. 1974. The Colville River and the Beaufort Sea: Some Interactions. *In:* Reed, J. C. & Sater, J. E. (eds) *The Coast and Shelf of the Beaufort Sea*. Arctic Institute of North America, Arlington, 513–540.

Appendix 1. *Arctic continental slopes polygon statistics*

Polygon no.	Flow regime	Late Quat. shelf edge ice	Mean slope	Max. slope	St. Dev. slope	Roughness (unitless)	Troughs	Shelf width (km)
1	C	Yes	0.97°	10.8°	0.73°	7.7	1	218
2	C	Yes	0.82°	2.9°	0.46°	5.1	1	252
3	D	Yes	2.46°	9.6°	1.34°	20.6	1	126
4	D	Yes	4.02°	23.3°	3.12°	42.5	–	58
5	C	Yes	1.04°	7.4°	0.76°	9.0	1	245
6	C	Yes	1.00°	5.7°	0.79°	9.0	1	223
7	C	Yes	1.65°	9.6°	0.93°	15.4	2	137
8	D	Yes	2.57°	9.1°	1.18°	25.2	1	85
9	D	Yes	2.50°	10.8°	1.36°	21.7	2	67
10	D	Yes	1.58°	10.2°	1.47°	12.6	–	83
11	D	Yes	3.94°	31.0°	3.52°	33.5	–	108
12	C	Yes	1.80°	13.5°	1.49°	13.4	1*	224
13	D	Yes	2.22°	9.6°	1.72°	13.4	1*	206
14	C	Yes	2.02°	14.6°	1.74°	13.9	1	155
15	C	Yes	1.69°	8.0°	0.94°	12.7	2	188
16	C	Yes	1.73°	6.8°	1.29°	10.6	1*	118
17	C	Yes	1.85°	6.3°	1.17°	10.6	2	124
18	?	Yes	1.66°	6.8°	1.22°	9.3	–	155
19	–	Ice Free	1.22°	4.0°	0.80°	6.7	2	241
20	–	Ice Free	1.76°	7.4°	1.34°	10.6	–	312
21	–	Ice Free	2.10°	8.0°	1.50°	14.9	–	339
22	–	Ice Free	1.34°	4.6°	0.77°	8.4	–	377
23	–	Ice Free	1.48°	5.1°	0.97°	11.5	–	337
24	–	Ice Free	1.32°	4.6°	0.91°	7.3	–	314
25	–	Ice Free	0.84°	4.6°	0.65°	4.8	–	389
26	–	Ice Free	2.89°	19.8°	2.06°	32.2	–	207
27	–	Ice Free	2.96°	14.6°	1.85°	29.9	–	133
28	–	Ice Free	2.41°	9.6°	1.90°	23.1	–	133
29	–	Ice Free	1.06°	10.2°	1.04°	6.4	1	190
30	–	Ice Free	0.75°	4.6°	0.46°	5.8	1	235
31	D	Yes	1.24°	10.8°	1.23°	10.8	2	202
32	Ice Shelf	Yes	1.46°	6.3°	1.04°	7.9	1	216
33	?	Yes	1.18°	7.4°	1.04°	9.8	–	205
34	D	Yes	1.48°	9.1°	1.29°	9.1	–	217
35	C	Yes	1.33°	5.7°	0.68°	11.4	2	201
36	C/D	Yes	1.50°	8.5°	0.89°	12.6	2	197
37	C/D	Yes	1.64°	6.8°	1.13°	15.1	–	145
38	C/D	Yes	1.55°	8.5°	1.55°	10.8	–	111
39	C/D	Yes	1.61°	7.4°	1.29°	10.6	–	157
40	C/D	Yes	1.65°	6.8°	1.36°	26.5	–	140
41	–	Ice Free	3.57°	11.9°	2.36°	21.6	–	148
42	–	Ice Free	2.74°	12.4°	2.14°	27.8	–	272
43	–	Ice Free	2.88°	11.3°	2.04°	15.7	–	328
44	–	Ice Free	2.23°	11.9°	1.28°	15.3	–	234
45	–	Ice Free	2.39°	9.6°	1.56°	13.5	1	149
46	C	Yes	1.97°	7.4°	1.36°	15.2	–	149
47	C	Yes	1.88°	6.3°	1.10°	20.7	1	122
48	D	Yes	2.02°	6.8°	1.48°	9.4	–	88
49	C	Yes	0.92°	8.0°	1.05°	10.8	–	149
50	D	Yes	1.47°	5.1°	0.84°	7.1	1	212
51	C	Yes	1.08°	11.3°	0.91°	7.6	–	206
52	C	Yes	0.90°	9.1°	0.80°	9.5	–	228
53	C	Yes	1.07°	4.0°	0.62°	13.2	–	145
54	D	Yes	1.29°	7.4°	0.86°	9.4	–	128
55	D	Yes	1.03°	4.0°	0.50°	12.2	–	135
56	D	Yes	1.24°	9.6°	1.02°	7.1	–	140

Appendix 1. *continued.*

Polygon no.	Flow regime	Late Quat. shelf edge ice	Mean slope	Max. slope	St. Dev. slope	Roughness (unitless)	Troughs	Shelf width (km)
57	C	Yes	0.65°	9.1°	0.60°	4.4	–	115
58	C	Yes	0.61°	6.3°	0.84°	8.7	–	112
59	C	Yes	1.02°	8.0°	0.87°	9.1	–	303
60	D	Yes	1.25°	5.7°	1.11°	7.1	1	184
61	C	Yes	1.15°	5.1°	0.97°	10.5	1	210
62	D	Yes	1.48°	7.4°	1.09°	11.4	1	194
63	C/D	Yes	1.40°	8.5°	1.45°	9.5	1	183
64	C/D	Yes	1.50°	7.4°	1.17°	10.6	–	69
65	C/D	Yes	1.52°	8.5°	1.39°	13.5	–	96
66	C/D	Yes	1.67°	10.2°	1.42°		–	91

Polygon no. refers to the numbering scheme in Figure 5.
Flow regime refers to the dominance of convergent, C, or divergent, D, ice flow at the shelf edge terminus.
Late Quat shelf edge ice lists whether or not we assume glaciation to the shelf edge at any time during the Late Quaternary (last 130 ka).
Mean, Max and Standard deviation slope are statistics for the entire polygon.
Roughness is the value for surface roughness of the sea floor within the polygon using a high-pass filter (see below and text).
Troughs refers to the number of troughs that are observed to be adjacent to the polygon.
Shelf width is the average distance to land from the polygon edge.
* Not used in analysis due to questionable quality of bathymetry data.

High-Pass Filter definition used for roughness estimation:

$$\frac{1}{9} \times \left(\frac{-S\,(x_i \times w_i)}{n} \right)$$

where,
x_i = cells in the 3 × 3 window
w_i = weight assigned to cells in window
n = number of cells in window (9)

The 3 × 3 kernel for cell weights consists of a central cell with a value of 17 and a value of –1 for the eight surrounding cells.